

# A Method for Unsupervised Change Detection and Automatic Radiometric Normalization in Multispectral Data

A. A. Nielsen <sup>a</sup>, M. J. Canty <sup>b</sup>

<sup>a</sup> Technical University of Denmark, National Space Institute, Building 321, DK-2800 Lyngby, Denmark – aa@space.dtu.dk

<sup>b</sup> Jülich Research Center, Institute for Bio- and Geoscience, IBG-3: Agrosphere, D-52425 Jülich, Germany – m.canty@fz-juelich.de

**Abstract** – Based on canonical correlation analysis the iteratively re-weighted multivariate alteration detection (MAD) method is used to successfully perform unsupervised change detection in bi-temporal Landsat ETM+ images covering an area with villages, woods, agricultural fields and open pit mines in North Rhine-Westphalia, Germany. A link to an example with ASTER data to detect change with the same method after the 2005 Kashmir earthquake is given. The method is also used to automatically normalize multitemporal, multispectral Landsat ETM+ data radiometrically. IDL/ENVI, Python and Matlab software to carry out the analyses is available from the authors' websites.

**Keywords:** canonical correlation analysis, multivariate alteration detection, MAD, IR-MAD, iMAD.

## 1. INTRODUCTION

The detection of change over time is a very important aspect of the analysis of digital satellite imagery. Many methods are available to carry out this type of analysis (Coppin et al., 2004). One such method is the iteratively re-weighted multivariate alteration detection (IR-MAD or iMAD) algorithm (Nielsen et al., 1998, Nielsen, 2007, Canty, 2010) which may be used for unsupervised change detection in multi- and hyperspectral remote sensing imagery as well as for automatic radiometric normalization of such multitemporal image sequences (Yang and Lo, 2000, Furby and Campbell, 2001, Du et al., 2002, Canty et al., 2004, Canty and Nielsen, 2008, Canty, 2010). Simple spectral band-by-band differences for simple change detection make sense only when the data are calibrated or at least normalized to the same scale and zero. It is often difficult to carry out such normalization especially for historical data where no auxiliary information on atmospheric conditions or instrument settings exists. In this paper the MAD method is applied to multispectral Landsat ETM+ data to carry out unsupervised change detection between acquisitions at two time points and to automatically normalize the data at the first time point to that of the second time point. Also, a link to an example with ASTER data to detect change after the 2005 Kashmir earthquake is given.

## 2. METHOD

The idea in the IR-MAD method is: rather than ordering the data by wavelength we order them by a measure of similarity, here correlation. This is done by means of an established multivariate statistical technique, namely canonical correlation analysis (CCA, Hotelling, 1936). Much like principal component analysis CCA constructs new orthogonal variables from the original ones. CCA finds two sets of linear combinations of the original variables, one for each time point. The first two linear combinations are the ones with the largest correlation. This correlation is called the first or leading canonical correlation and the two linear combinations are

called the first or leading canonical variates. The second two linear combinations are the ones with the largest correlation subject to the condition that they are orthogonal to the first canonical variates. This correlation is called the second canonical correlation and the two linear combinations are called the second canonical variates. Higher order canonical correlations and canonical variates are defined similarly.

The pair-wise differences between the canonical variates which are as similar as they can get are the change variables; these differences are termed the MAD variates or MADs for short. Because these MADs are orthogonal, ideally different types of change will be associated with different canonical variates and MAD variates. Basing the MAD transform on CCA ensures independence of linear and affine scaling of the original data.

Properly normed to unit variance, the sum of the squared MAD variates ideally will follow a chi squared distribution with as many degrees of freedom as we have spectral bands. This may be used to calculate a measure of probability of no-change. This in a series of iterations is used to place increasing weight on the no-change observations to obtain an increasingly better background of no-change against which to detect change. Also, the no-change observations may be used in orthogonal regression (also known as total least squares) which allows for uncertainties in both or all variables involved, to obtain automatic radiometric normalization of image time series.

## 3. DATA

The method is applied to Landsat ETM+ data covering villages, woods, agricultural areas and open pit mines in North Rhine-Westphalia, Germany. Also, a link to an example with ASTER imagery for detection of landslides in the aftermath of the 2005 earthquake in Kashmir is given.

### 3.1 Landsat ETM+ Data, Jülich, Germany

Landsat ETM+ data covering villages, woods, agricultural areas and open pit mines in the Rur catchment basin centered on the town Jülich, Germany, from 26 June and 29 August 2001 are subjected to the IR-MAD change analysis (the thermal band is excluded from the analysis).

Figures 1 and 2 show Landsat ETM+ bands 4, 5 and 3 acquired at 26 June and 29 August 2001 as RGB. The images are 1000 by 1000 28.5 meter pixels. Figure 3 shows the development of the six canonical correlations over the iterations. After approximately 25 iterations the method seems to home in on the no-change observations and then it stabilizes.

Figure 4 shows a scatter plot of the leading canonical variates for the two time points. This shows no-change pixels along the line  $y=x$  and change pixels off that line. Figure 5 shows the same scatter plot after iterations, and we see that a much better discrimination between change and no-change is achieved (the "bump" off the line  $y=x$  are the change pixels).

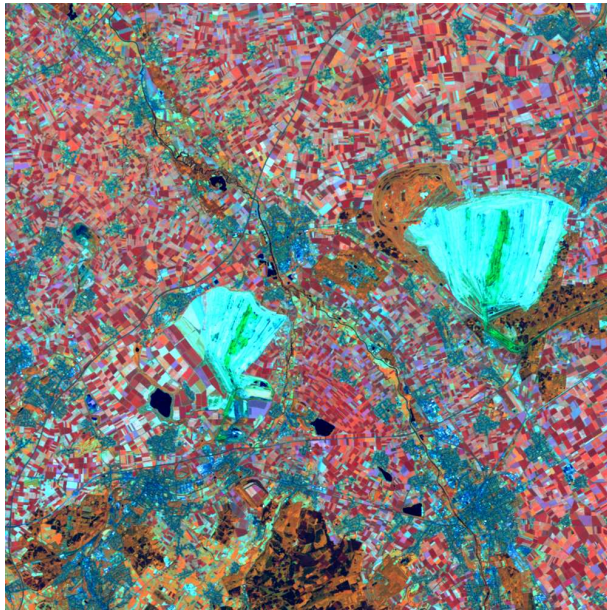


Figure 1. Landsat ETM+ data, Jülich, Germany, 26 Jun 2001.

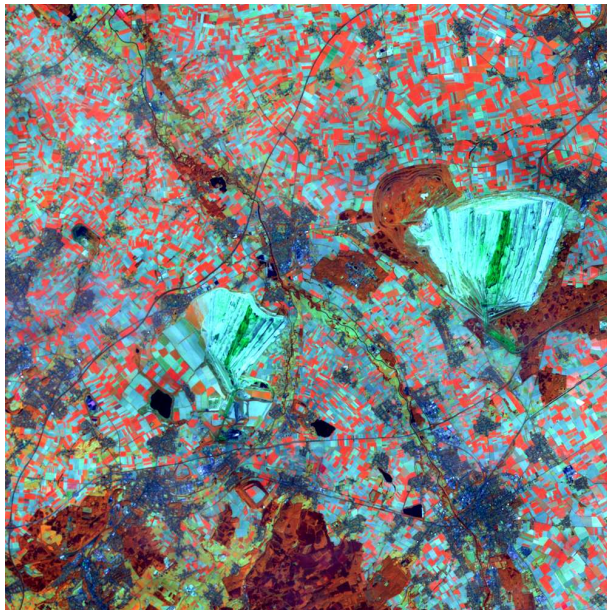


Figure 2. Landsat ETM+ data, Jülich, Germany, 29 Aug 2001.

Figure 6 shows the three IR-MAD variates corresponding to the highest canonical correlations as RGB. No-change regions (primarily villages and woods) are the grayish, structureless areas, change regions (mainly agricultural fields and open pit mines) have structure and are in saturated colours (including black and white if present). The colours indicate the type and direction of change (primarily maturing sugar beet and corn crops and grain harvesting).

Figure 7 shows the so-called chi squared image where black indicates no-change and white change. The brightest pixels and hence the largest amount of change is associated with agricultural activities.

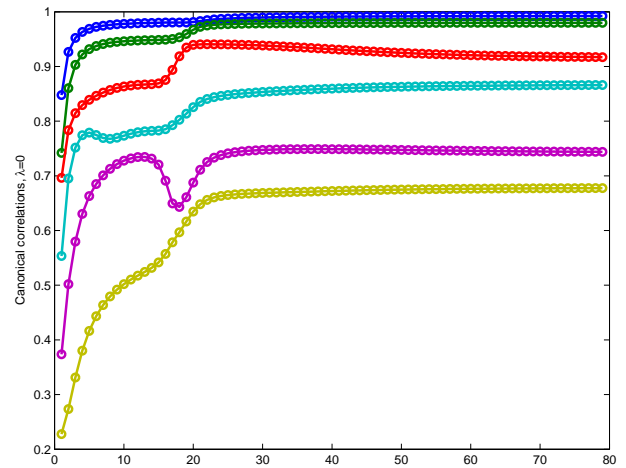


Figure 3. Canonical correlations over iterations.

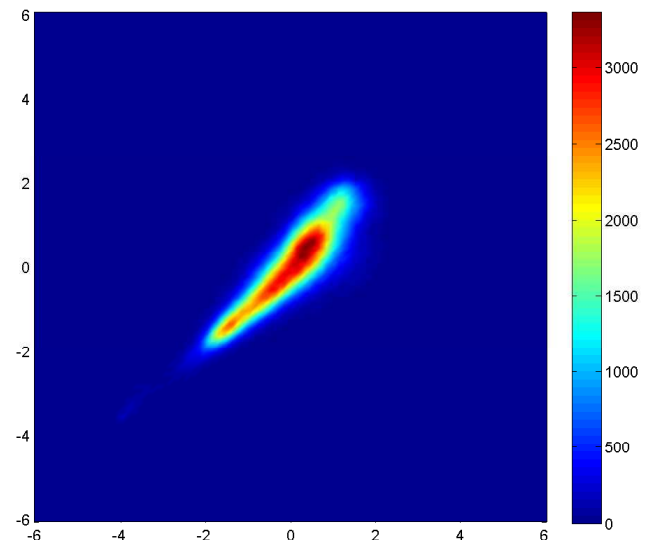


Figure 4. Scatter plot of canonical variates 1.

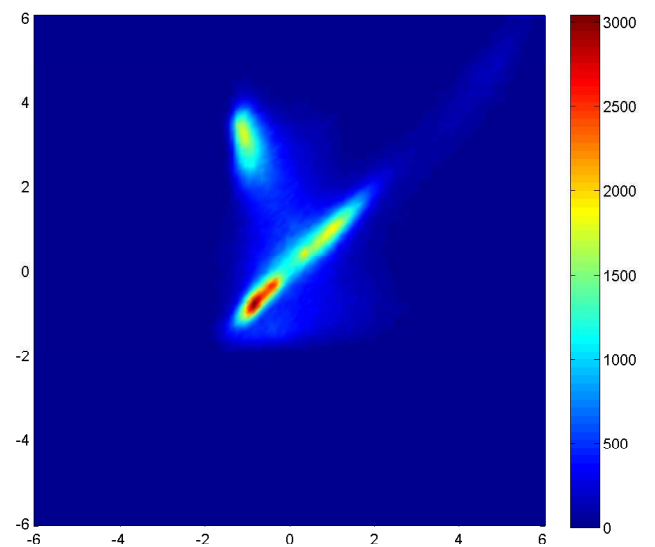


Figure 5. Scatter plot of iterated canonical variates 1.



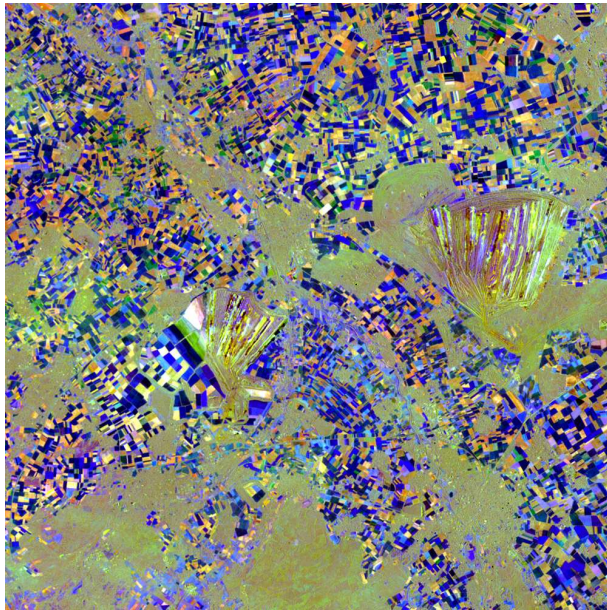


Figure 6. Landsat ETM+, Jülich, Germany, IR-MAD.

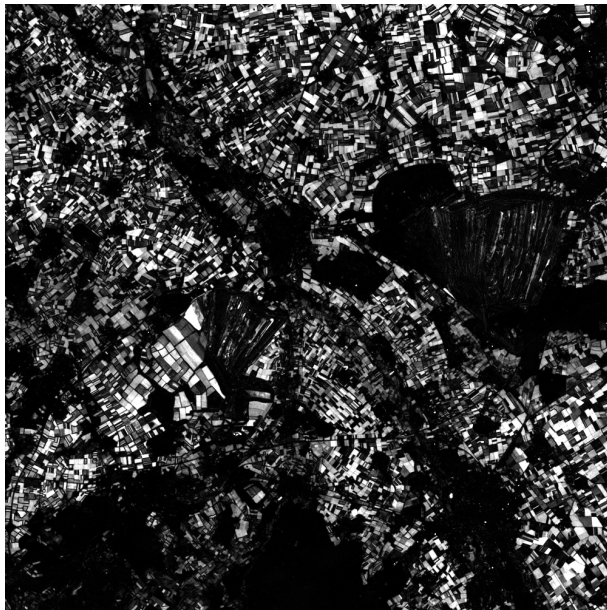


Figure 7. Landsat ETM+, Jülich, Germany, chi squared image.

### 3.2 Automatic Radiometric Normalization

As mentioned the no-change observations detected by the iMAD method may be used in orthogonal or total least squares regression to automatically normalize a series of multispectral images to the same reference. To do this we randomly divide the no-change observations between the two time points (here the pixels with probability of no-change greater than 0.95) into a training set (here consisting of 1,211 pixels) and a test set (here consisting of 578 pixels). If we normalize the training pixels from 26 June to the data from 29 August (which is then the reference) orthogonal regression gives the calibration lines in Figures 8 (for the training data) and 9 (for the test data); as an example band 5 is shown. Although the calibration line is based on the training data only, after calibration the test data fit the line  $y=x$  neatly.

Intercepts and slopes with standard errors for all six bands are shown in Table A.  $t$ -values and probabilities for obtaining a higher value of  $|t|$  are included (standard errors should be low,  $t$ -values high and probabilities close to 0, normally we say  $p < 0.05$ ).

Table B gives paired  $t$ -tests for equal means for the test data after normalization (differences and  $t$ -values should be close to 0 and probabilities high – the closer to 1 the better, normally we say  $p > 0.05$ ). Table C gives  $F$ -tests for equal variances of the test data after normalization ( $F$ -values should be close to 1 and probabilities high – the closer to 1 the better, normally we say  $p > 0.05$ ).

Since the variables at both time points are associated with uncertainty orthogonal regression must be used here. In fact, what is called reference data and what is called uncalibrated data is arbitrary.

See also <http://fwenvi-idl.blogspot.com/2009/07/normalizing-images.html>.

### 3.3 ASTER Data, Kashmir, Pakistan

This example is not described in detail here. Instead see <http://fwenvi-idl.blogspot.com/2009/06/detecting-changes.html> which illustrates the application of the MAD method to detect mudslides in the aftermath of the disastrous earthquake of 8 October 2005 centered near the city of Muzaffarabad in Pakistan-administered Kashmir. The link also gives a neat Google Earth projection of the change detected. The region lies in the area of collision of the Eurasian and Indian tectonic plates. According to the United States Geological Survey (USGS) this earthquake had a magnitude of (at least) 7.6 on the moment magnitude scale (denoted MMS or  $M_w$ ) making it similar in size to the infamous 1906 earthquake in San Francisco, USA. The data applied are the three VNIR 15 meter pixels ASTER bands 1, 2 and 3N over the area acquired on 5 September and 27 October 2005.

The Kashmir earthquake caused the death of more than 75,000 people and enormous damage to housing and infrastructure, see [http://en.wikipedia.org/wiki/2005\\_Kashmir\\_earthquake](http://en.wikipedia.org/wiki/2005_Kashmir_earthquake).

## 4. CONCLUSIONS

We have demonstrated how the iterated scheme in the MAD method homes in on the no-change observations giving a very good discrimination between change and no-change regions. We have also shown how the no-change observations may be used in orthogonal regression (or total least squares) to obtain automatic radiometric normalization of image time series including statistical tests for equal means and variances after normalization.

Post-processing of the MAD variates by means of kernel versions of principal components (Schölkopf et al., 1998) or maximum autocorrelation factors/minimum noise fractions (Green et al., 1988, Nielsen, 2011) may be useful.

Sometimes both change detection and normalization by the MAD method fail because not enough no-change pixels can be found. In these cases it is often advantageous to establish the transformation in a sub-area or region of interest only and then apply the transformation to the entire scene.

IDL/ENVI, Python and Matlab software to carry out the MAD based analyses is available from the authors' websites.

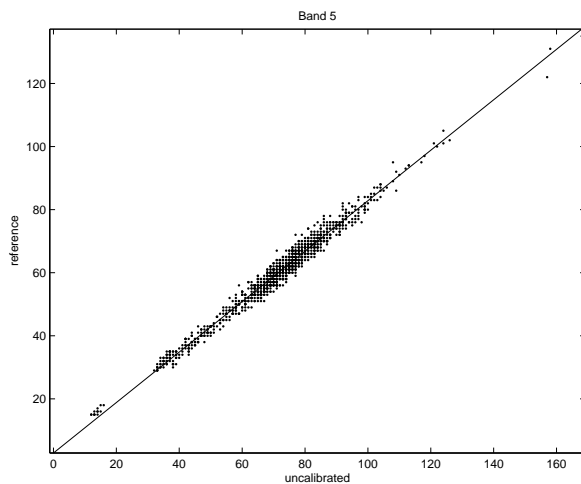


Figure 8. Calibration line for band 5, training data.

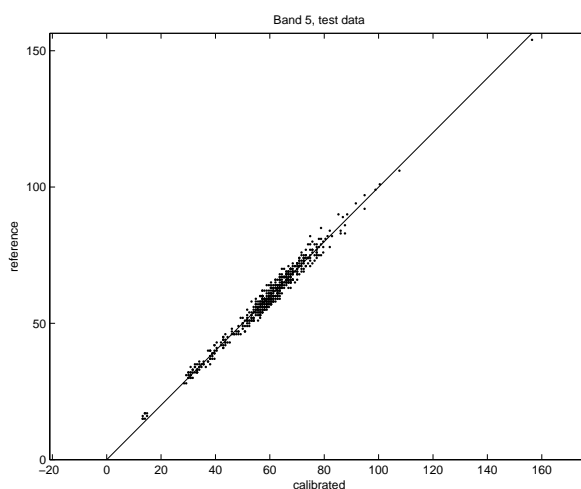


Figure 9. After calibration, band 5, test data; line is  $y=x$ .

Table A. Intercepts and slopes for all bands, training data only.

Band	Intercept	Std.err.	t	P	Slope	Std.err.	t	p
1	1.1249	0.4820	2.33	0.02	0.8679	0.0063	138	0.00
2	2.0523	0.2836	7.24	0.00	0.8408	0.0048	174	0.00
3	6.6036	0.1900	34.76	0.00	0.7916	0.0037	211	0.00
4	4.3352	0.4247	10.21	0.00	0.6996	0.0048	146	0.00
5	2.8539	0.2584	11.05	0.00	0.7999	0.0035	226	0.00
7	6.1150	0.1037	58.97	0.00	0.7554	0.0024	317	0.00

Table B. Paired t-tests for equal means after normalization, test data.

Band	Uncorr.	Normalized	Ref.	Diff.	t	p
1	75.87	66.97	66.78	0.20	2.52	0.01
2	57.83	50.68	50.56	0.11	1.60	0.11
3	48.10	44.68	44.54	0.14	1.65	0.10
4	85.21	63.95	64.00	-0.04	-0.26	0.80
5	70.21	59.01	58.92	0.09	0.99	0.32
7	39.66	36.07	35.99	0.08	1.42	0.16

Table C. F-tests for equal variances after normalization, test data.

Band	Uncorr.	Normalized	Ref.	F	p
1	80.38	60.55	64.83	0.9339	0.41
2	104.35	73.77	79.10	0.9326	0.40
3	243.35	152.46	160.54	0.9497	0.54
4	566.87	277.47	294.76	0.9413	0.47
5	324.67	207.72	209.06	0.9936	0.94
7	291.26	166.19	169.74	0.9791	0.80

## REFERENCES

- M.J. Canty, *Image Analysis, Classification and Change Detection in Remote Sensing, with Algorithms for ENVI/IDL*, Second Revised Edition, Taylor & Francis, CRC Press, 2010.
- M.J. Canty and A.A. Nielsen, "Automatic radiometric normalization of multitemporal satellite imagery with the iteratively re-weighted MAD transformation," *Remote Sensing of Environment* **112**(3), pp. 1025-1036, 2008. <http://www.imm.dtu.dk/pubdb/p.php?5362>.
- M.J. Canty, A.A. Nielsen, and M. Schmidt, "Automatic radiometric normalization of multitemporal satellite imagery," *Remote Sensing of Environment* **91**, pp. 441-451, 2004. <http://www.imm.dtu.dk/pubdb/p.php?2815>.
- P. Coppin, I. Jonckheere, K. Nackaerts, and B. Muys, "Digital change detection methods in ecosystem monitoring: A review," *International Journal of Remote Sensing* **25**(9), pp. 1565-1596, 2004.
- Y. Du, P.M. Teillet, and J. Cihlar, "Radiometric normalization of multitemporal high-resolution images with quality control for land cover change detection," *Remote Sensing of Environment* **82**, pp. 123-134, 2002.
- S.L. Furby and N.A. Campbell, "Calibrating images from different dates to like-value counts," *Remote Sensing of Environment* **77**, pp. 186-196, 2001.
- A.A. Green, M. Berman, P. Switzer, and M.D. Craig, "A transformation for ordering multispectral data in terms of image quality with implications for noise removal," *IEEE Transactions on Geoscience and Remote Sensing* **26**(1), pp. 65-74, 1988.
- H. Hotelling, "Relations between two sets of variates," *Biometrika* **XXVIII**, pp. 321-377, 1936.
- A.A. Nielsen, "The regularized iteratively reweighted MAD method for change detection in multi- and hyperspectral data," *IEEE Transactions on Image Processing* **16**(2), pp. 463-468, 2007. <http://www.imm.dtu.dk/pubdb/p.php?4695>.
- A.A. Nielsen, "Kernel maximum autocorrelation factor and minimum noise fraction transformations," *IEEE Transactions on Image Processing*, in press, 2011. <http://www.imm.dtu.dk/pubdb/p.php?5925>.
- A.A. Nielsen, K. Conradsen, and J.J. Simpson, "Multivariate alteration detection (MAD) and MAF post-processing in multispectral, bi-temporal image data: New approaches to change detection studies," *Remote Sensing of Environment* **64**, pp. 1-19, 1998. <http://www.imm.dtu.dk/pubdb/p.php?1220>.
- B. Schölkopf, A. Smola, and K.-R. Müller, "Nonlinear component analysis as a kernel eigenvalue problem," *Neural Computation* **10**(5), pp. 1299-1319, 1998.
- X. Yang and C.P. Lo, "Relative radiometric normalization performance for change detection from multi-date satellite images," *Photogrammetric Engineering and Remote Sensing* **66**, pp. 967-980, 2000.